



HAL
open science

Conformation of substituted polyacetylenes in solution : relationship between electronic properties and local order

P. Garrin, J. Aimé, J. Fave, S. Ramakrishnan, G. Baker

► **To cite this version:**

P. Garrin, J. Aimé, J. Fave, S. Ramakrishnan, G. Baker. Conformation of substituted polyacetylenes in solution : relationship between electronic properties and local order. *Journal de Physique II*, 1992, 2 (3), pp.529-546. 10.1051/jp2:1992147 . jpa-00247648

HAL Id: jpa-00247648

<https://hal.science/jpa-00247648>

Submitted on 4 Feb 2008

HAL is a multi-disciplinary open access archive for the deposit and dissemination of scientific research documents, whether they are published or not. The documents may come from teaching and research institutions in France or abroad, or from public or private research centers.

L'archive ouverte pluridisciplinaire **HAL**, est destinée au dépôt et à la diffusion de documents scientifiques de niveau recherche, publiés ou non, émanant des établissements d'enseignement et de recherche français ou étrangers, des laboratoires publics ou privés.

Classification

Physics Abstracts

36.20 — 46.90 — 71.90

Conformation of substituted polyacetylenes in solution : relationship between electronic properties and local order

P. Garrin ⁽¹⁾, J. P. Aimé ^(1, *), J. L. Fave ⁽¹⁾, S. Ramakrishnan ⁽²⁾ and
G. L. Baker ⁽³⁾

⁽¹⁾ Groupe de Physique des Solides, Université Paris VII, Tour 23, 2 place Jussieu, 75251 Paris Cedex 05, France

⁽²⁾ Dept of Inorganic and Physical Chemistry, Indian Institute of Science, Bangalore-560012, India

⁽³⁾ Bellcore, 331 Newman Springs Road, Red Bank, New-Jersey 07701-7040, U.S.A.

(Received 11 September 1991, revised 28 October 1991, accepted 15 November 1991)

Résumé. — Nous présentons une étude de la conformation en solution du polyphénylacétylène et du poly(2-octyne). Ces deux polymères ont des comportements très différents : la solution de polyphénylacétylène est rouge alors que celle de poly(2-octyne) est transparente et les longueurs statistiques mesurées sont respectivement 45 et 135 Å. L'étude de ces deux systèmes nous permet de déduire que la fluctuation de courbure joue un rôle mineur sur la localisation des électrons π du squelette. Elle nous permet également de montrer que la torsion entre unités monomères est responsable de la localisation des électrons π et d'expliquer la conformation statistique des chaînes.

Abstract. — A study of the chain conformation in solutions of polyphenylacetylene and poly(2-octyne) has been performed. The two polymers differ in many ways : polyphenylacetylene gives a red solution while poly(2-octyne) is transparent and, a marked difference on the chain rigidity is observed : the statistical length are 45 Å and 135 Å respectively. From the study of these two systems, one deduces that curvature fluctuations play a minor role on the π electrons localization, and that the torsion between monomer units is the pertinent parameter to understand the chain conformation and the π electrons localization.

1. Introduction.

Conjugated polymers with large molecular weights can be solubilized in common organic solvents by adding appropriate substituents. Most exhibit thermochromism and solvatochromism, which has stimulated extensive studies on the relation between optical properties and chain conformation. Moreover homogeneous solutions of macromolecules can provide the opportunity to study the single chain properties.

The notion of conjugation length is widely used to explain the visible absorption and the Resonant Raman Scattering (R.R.S.) results [1, 2]. It is a useful phenomenological parameter

(*) *Present address* : Laboratoire de Cristallographie et Physique Cristalline. Université Bordeaux I, 351, cours de la Libération, 33405 Talence Cedex, France.

describing electron delocalization along the backbone, and is related to the average overlap between π electrons orbitals. Since the overlap can be decreased by curvature or torsional fluctuations, the location of the maximum optical absorption in the visible spectrum as well as its broad and structureless character is explained as a direct consequence of the statistical conformation of the polymer [3]. On the other hand, the role of conjugation was considered of primary importance for understanding stiffness at the local scale, suggesting that conjugated polymers should exhibit greater rigidity than saturated ones [4, 5]. This concept was in part supported by the results obtained from the polydiacetylenes P4BCMU, P3BCMU and PTS12 [6, 7].

Conversely, recent studies have shown that the substituents and the torsion between monomer units play a key role in understanding the statistical conformation [8, 9] and an increasing amount of theoretical work has paid special attention to the effects of torsional fluctuations, emphasizing their influence on the π electrons delocalization [10-13].

In this paper we describe experiments aiming to establish as accurately as possible the description of the chain statistics, to predict its link with the π electrons delocalization. Small Angle Neutron Scattering (SANS) was used to provide structural information at intermediate and local scales, that is between 200 and 10 Å. Then the chain conformation was related to visible absorption spectroscopy and R.R.S. results. Several studies have already been carried out with polydiacetylene and polythiophene derivatives [7, 14].

Here we focus our work on substituted polyacetylenes whose generic formula is $(RC = CR')_n$. In this note, we give two examples. One is polyphenylacetylene (hereafter abbreviated PPA), where $R = H$ and $R' = C_6H_5$, for which NMR experiments suggested a helical structure which was not confirmed by R.R.S. [15-17]. The second concerns the poly(2-octyne), where $R = CH_3$ and $R' = CH_2)_4CH_3$, as a model system.

2. Experimental section.

2.1 SAMPLE DESCRIPTION. — Using tungsten hexachloride (WCl_6) and molybdenum pentachloride ($MoCl_5$) catalysts, Masuda *et al.* [15] polymerized PPA to a molecular weight larger than 10^4 . With these two catalysts, polymerization of soluble polyacetylenes with various substituents was achieved [15]. Numerous parameters govern the polymer properties : the catalyst, cocatalyst and even the solvent used for the polymerization. Here the synthesis has been done in toluene with WCl_6 and the cocatalyst $SnMe_4$, instead of $WCl_6/Sn\Phi_4$ used by Abe *et al.* [16]. The PPA solution absorbs at longer wavelength (paragraph 2.3.1) than the one obtained by Abe *et al.* [16]. A molecular weight of 49 000 with a polydispersity (M_w/M_n) of 1.35 have been measured by G.P.C.

For the poly(2-octyne) sample, the molecular weight is $M_w = 675\ 000$ with a polydispersity 1.8. The light scattering study yielded a radius of gyration $R_G = 520 \pm 20$ Å. In spite of the conjugated backbone, the solution was transparent, showing the same optical properties as common saturated polymers.

2.2 SANS METHODOLOGY. — Neutron scattering experiments were performed at the Institut Laue-Langevin on the diffractometers D11, D17 and D16. The sample-detector distances and wavelengths used were 5 m and 8 Å, 3.46 m and 12 Å and 1 m and 4.56 Å, respectively for D11, D17 and D16, corresponding to the range $6 \times 10^{-3} \text{ \AA}^{-1} < q < 0.25 \text{ \AA}^{-1}$, where q is the scattering vector defined by :

$$q = \frac{4 \pi}{\lambda} \sin \left(\frac{\theta}{2} \right) \quad (1)$$

with θ the scattering angle and λ the neutron incident wavelength.

The macromolecules studied scatter isotropically in solution, thus an isotropic average on the data collected on the two-dimensional detector was performed. Then it was corrected from solvent background with the current routines available at I.L.L. and normalized to the scattering intensity given by a water cell [18]. Absolute measurement was thus obtained, providing a constraint which allowed accurate determination of the chain statistics. The scattering intensity $S(q)$ is the Fourier transform of the autocorrelation function of the monomer density $\langle \rho(r) \rho(0) \rangle$. Contributions of the density-density fluctuations within and between chains were also considered; the latter being due to interchain interaction gives a concentration dependence on the scattering function. In the Guinier range, i.e. for a radius of gyration of the macromolecule R_G , in the range $qR_G < 1$, the interchain interference was removed by using the Zimm extrapolation method. At a length scale smaller than the radius of gyration of the polymer R_G ($qR_G > 1$) intrachain correlations are measured, which are normally independent of the concentration in the diluted regime. This point has been checked in the whole q range in the present experiments.

When an isolated chain state is measured, it is often more convenient to use the scattering function normalized to the molecular weight of the chain :

$$g(q) = \frac{m}{K^2 c \mathcal{N}} S(q) = \frac{M_w}{m} P(q) \quad (2)$$

where $P(q)$ is defined such that $P(0) = 1$, m is the molar mass of the monomer unit, \mathcal{N} is Avogadro's number and K is the contrast factor defined by :

$$K = \sum_i a_i^m - \frac{v_m}{v_s} \sum_i a_i^s \quad (3)$$

where v_s and v_m are the molar volumes of the solvent and monomer units and a_i^k is the coherent scattering length of the atom i . Note that in equation 3 the monomer unit is assumed to be a point scatterer with a scattering length density obtained from the average of all atomic contributions.

2.2.1 Scattering function of chain with statistical length. — Considering a chain as an infinitely thin thread, we focus attention on conformation at the local scale. In other words, we are interested in the asymptotic regime of the scattering function, that is, $g(q) \propto q^{-\alpha}$ for $q \rightarrow \infty$. For simplicity we consider two asymptotic laws : a q^{-2} law for the Gaussian coil (with an excluded volume effect and for very large chains, the exponent is given by $\alpha \approx 1/0.6$ [19]) and a q^{-1} law for the rod. The purpose of the dimensionless scattering function $g(q)$ is to obtain the scattering density of the macromolecule in the asymptotic regime. For the case of the rod conformation, defining M_L as the mass per unit length, the limit of $g(q)$ is given by :

$$\lim_{q \rightarrow \infty} qg(q) = \frac{\pi M_L}{m} = \frac{\pi}{u} \quad (4)$$

where u is the monomer unit length. Therefore the plateau height in a $qg(q)$ plot gives the linear density of the macromolecule in a rod conformation. For an actual wormlike chain, the angular correlation along the backbone can be large enough such that a rigid conformation is observed. The rigidity is measured by the statistical length b (or the persistence length, which is half of the statistical length) and defined by equation (5) [20] :

$$\langle \mathbf{t}_1 \cdot \mathbf{t}_2 \rangle = \exp \left(- \frac{2|l_1 - l_2|}{b} \right) \quad (5)$$

where the vectors \mathbf{t}_i are unit vectors tangent to the backbone at the curvilinear abscisse l_i . Therefore, one can expect that for a fairly rigid polymer, we can observe different scattering regimes depending on the scale at which the scattering function is measured. Actually, Yoshisaki and Yamakawa (Y.Y. model) have demonstrated that wormlike chains with finite contour lengths do not exhibit a q^{-2} behavior at low q values [21]. They proved that if a worm-like chain shows a q^{-2} behavior, it should correspond to a chain with a persistence in curvature, that is a helical worm-like chain. For a worm-like chain, the asymptotic behavior is described by equation (6) [21] :

$$\lim_{q \rightarrow \infty} q^2 g(q) = \frac{\pi q}{u} + \frac{C(N)}{ub} \quad (6)$$

where u is the monomer unit length, N the number of monomer units in the chain, with $C(N) = -2N^{-1}$ for the rod and $C(\infty) = 4/3$ for an infinite worm-like chain [22]. More quantitatively such a behavior will be observed for $qb \geq 7$ as long as the ratio L/b (where $L = Nu$ is the contour length) is larger than 2 [7].

2.2.2 Effect of chain thickness. — Because conjugated polymers need large substituents to be solubilized, they differ markedly from common polymers such as polyisoprene and polystyrene. In most practical cases, it is not enough to have the general variation of the scattering function for an infinitely thin thread. As we show in part 3, the finite lateral dimensions of the chain modify the structure factor at large q . The general form of the scattering function for chain with finite lateral dimensions can be approximated by equation (7) [23, 24] :

$$g(q) = g_0(q) \Phi(q) \quad (7)$$

where $g_0(q)$ is now the structure factor corresponding to the infinitely thin thread and $\Phi(q)$ describes the effect of the substituent side-groups. Approximate expressions for $\Phi(q)$ are often sufficient for describing the whole scattering vector range investigated [23, 24]. A well known approach is to use the Guinier approximation. Setting R_c^2 , the mean square radius of gyration for the lateral dimension, for $q < \frac{1}{R_c}$ $\Phi(q)$ is written

$$\Phi(q) = \exp \left(- \frac{q^2 R_c^2}{2} \right) . \quad (8)$$

To describe the scattering function at larger q values, a more precise description of the cross section is needed. To address this a simple geometrical form can be used e.g. a cylinder, a ribbon, or a chain with helical cross sections. This will be discussed in more detail in 3.1.3.

2.3 RESULTS.

2.3.1 Optical and R.R.S. results. — It has been reported [15] that films of PPA are not very stable. Degradation effects are observed in films kept at room temperature for about three months. In solution, the PPA samples degrade in a much shorter time : the solutions become colorless within a day at room temperature. In order to prevent degradation, the experiments were performed at 5 °C. For the stable poly(2-octyne), all experiments were performed at room temperature.

The poly(2-octyne) absorbs in the U.V. range (below 280 nm). For PPA, the solution is red : the absorption maximum is located at 450 nm with a tail up to 650 nm (Fig. 1). The absorption spectrum suggests a broad distribution of conjugation lengths corresponding to an electron delocalization much larger than for poly(2-octyne).

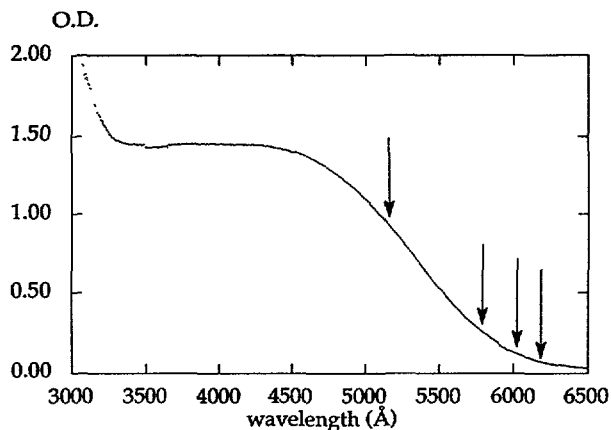


Fig. 1. — Visible Absorption spectrum of PPA in toluene. Arrows indicate the excitation wavelength used for R.R.S.

R.R.S. is often used to analyze the backbone structure and distribution of conjugation lengths. For samples with substituent side-groups a much more complicated analysis is required [17], but the technique was still useful for comparing local structure in the film and the solution. The available excitation wavelengths of our lasers were between 4 579 Å and 6 400 Å, too far from the poly(2-octyne) absorption to be still resonant. For PPA, Raman spectra have been obtained at different wavelengths both for the film and the solution (Fig. 2). In studies of excitation wavelength, an inversion of the intensities of the two peaks

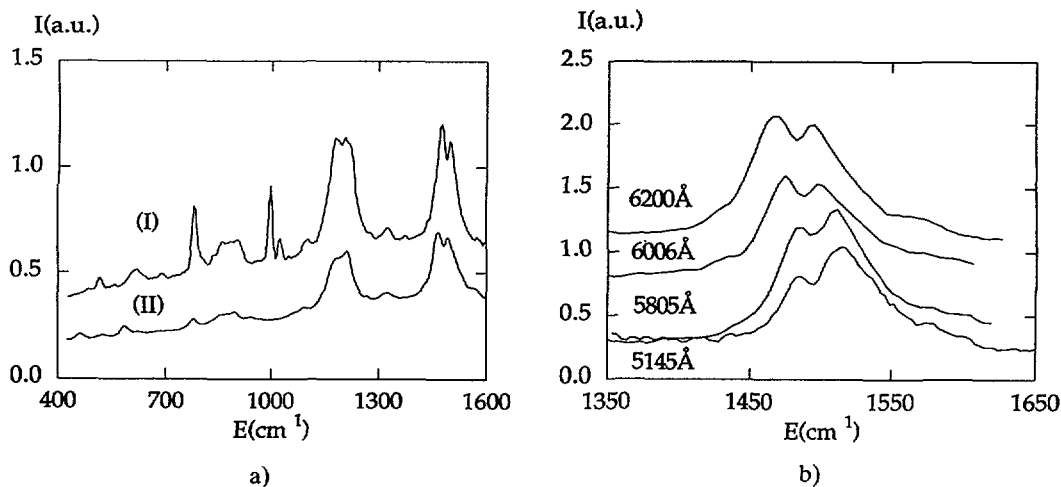


Fig. 2. — a) Raman spectrum of PPA in solution (I) and film (II). Additional sharp vibrational lines in solution correspond to the solvent toluene. b) Evolution of the double bonds frequency as a function of the incident wavelength in solution.

around $1\,500\text{ cm}^{-1}$ (C=C stretching) was observed. Also, the spectra are nearly identical in film and solution, suggesting that solubilization does not induce isomerisation process or drastic changes in the chain curvature or rotation between monomer units. Our spectra are reminiscent of those of Batchelder *et al.* obtained for a similar sample that they called PPA II [17], except for the light difference between the films and solutions : we have found that the films spectral maxima are at lower frequencies suggesting a higher degree of order. Without taking into account coupling between the phenyl and main chain vibrations, they proposed a *trans*-cisoid structure ; however, they recognized that this analysis was not entirely conclusive, the Raman results being seemingly in contradiction with the IR and NMR data.

2.3.2 SANS results. — After one hour of collecting data, we observed a decrease of the scattering intensity at low q values at room temperature for PPA (Fig. 3). This observation was directly related to a drastic loss of molecular weight. The degradation process not only shortens the conjugation length as shown by the disappearance of the visible optical absorption, but also breaks the chain itself. Thus, in order to prevent sample degradation, the experiments were performed at $5\text{ }^\circ\text{C}$. At this temperature, degradation is controlled and we noticed only a slight decrease of the scattering intensity at low q after one day (Fig. 3). We thus discuss the measurements performed at $5\text{ }^\circ\text{C}$ keeping in mind that we do not have the same sample quality as for poly(2-octyne).

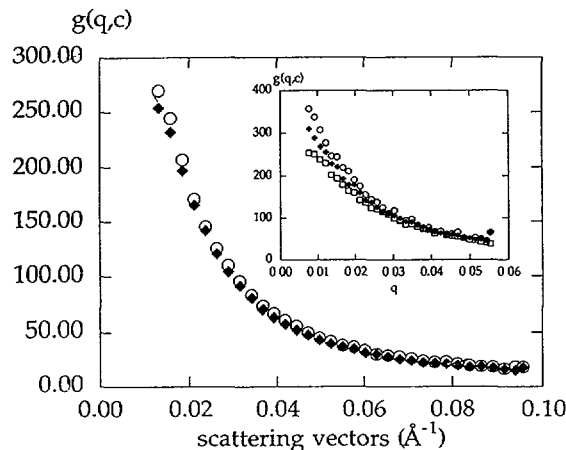


Fig. 3. — Decrease of the scattering intensity as a function of time, due to the degradation of the PPA chains in solution at $5\text{ }^\circ\text{C}$ (b) : (○) $t = 0$, (◆) after 10 hours. The inset figure corresponds to the room temperature measurements : (○) $t = 0$, (◆) after 6 hours, (□) after 12 hours.

The measured scattering functions for polyphenylacetylene and poly(2-octyne) samples are shown in figure 4. Except at the lowest value of the scattering vectors, $q = 6 \times 10^{-3}\text{ } \text{Å}^{-1}$, we do not observe any effect due to the concentration between 1.2 and $0.6 \times 10^{-3}\text{ g cm}^{-3}$. The scattering functions are corrected for the incoherent contribution of the atoms belonging to the chain. The main contribution comes from the incoherent cross-section of the protons, which can be significantly different from the value given in the table I [25]. In order to have an accurate estimation of the incoherent cross section of the protons, measurements at large scattering vectors ($q = 0.45\text{ } \text{Å}^{-1}$) were done. The contribution of the carbon atoms is negligible. Using equation (9),

$$S^{\text{inc}} \sim \frac{N^2 c}{4 \pi m} \sigma_{\text{H}}^{\text{inc}} n_{\text{H}} \quad (9)$$

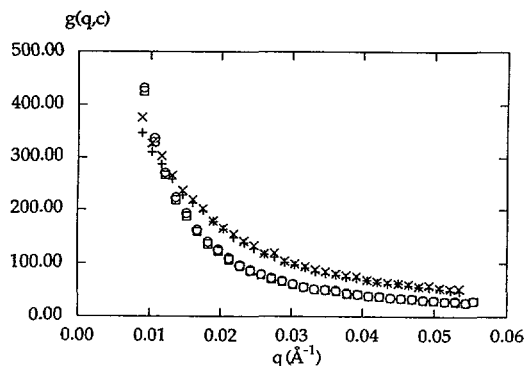


Fig. 4. — Scattering function of PPA and poly(2-octyne) at two concentrations. PPA : $c = 0.6 \text{ mg/cm}^{-3}$ (\times), $c = 1.2 \text{ mg/cm}^{-3}$ ($+$); poly(2-octyne) : $c = 1.2 \text{ mg/cm}^{-3}$ (\square), $c = 0.6 \text{ mg/cm}^{-3}$ (\circ).

Table I. — Helix parameters used for the refinement of the poly(2-octyne) scattering function. The parameters are given in Angström.

Monomer unit structure	P	L_T	aR	b	$\frac{L}{b}$
<i>trans</i> -transoid	20	6	1.78	135	110
	15	6.5	1.33	135	110
<i>cis</i> -transoid	15	6	1.72	135	102

where n_H is the number of protons in the monomer unit, gives an estimation of the $\sigma_H^{\text{inc}} \approx 100$ barns with the wavelength $\lambda' = 4.56 \text{ \AA}$ (much larger than the value found in the table : $\sigma_H^{\text{inc}} \sim 81$ barns).

The final scattering functions shown are obtained by subtracting the incoherent contribution 0.6 for poly(2-octyne) and 0.3 for PPA. This subtraction has a negligible effect at low q values, but it may change the curve significantly at large q . For example, for the poly(2-octyne) at $q = 0.05 \text{ \AA}^{-1}$ $g(q, c) = 30$, thus an incoherent contribution of about 2 %, while at $q = 0.2 \text{ \AA}^{-1}$ $g(q, c) = 3.1$, thus an incoherent contribution of about 20 %.

For a $qg(q)$ plot, with a polyacetylene in a *trans*-transoid conformation and using a monomer unit length $u = 2.43 \text{ \AA}$, the plateau height must be close to 1.29, while for a *cis*-transoid or a *trans*-cisoid conformation (Fig. 5) with $u = 2.61 \text{ \AA}$, it must be close to 1.20. The

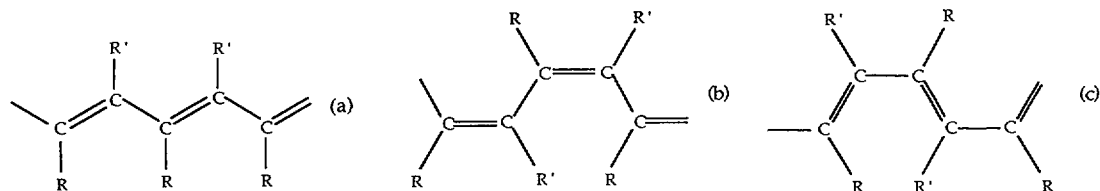


Fig. 5. — Different possible structures for the polyacetylene backbone : *trans*-transoid (a), *cis*-transoid (b), *trans*-cisoid (c).

difference between the two values is about 7.5 % which is approximately within the experimental error. As shown by equation (6), such a plateau will also be observed with a worm-like chain when the statistical length is sufficiently large.

In figures 6 and 7, the $qg(q, c)$ and $q^2g(q, c)$ plots are shown. For the case of poly(2-octyne), the $qg(q, c)$ plot does not show the expected value for the plateau height. The value measured is 1.48 : i.e., it is 15 % higher than the calculated value for the *trans*-transoid conformation and 23 % higher than the one for the *trans*-cisoid conformation. This discrepancy is much larger than the experimental accuracy in our measurements. For example the deuterated solvent height measured in various experiments (toluene, THF, DMF...) gives a difference of about 5 % from the calculated values. This sizeable difference is discussed in paragraph 3.

At large values of the scattering vector, one obtains a completely different behavior between PPA and poly(2-octyne) (Fig. 7). PPA shows a variation of the scattering function

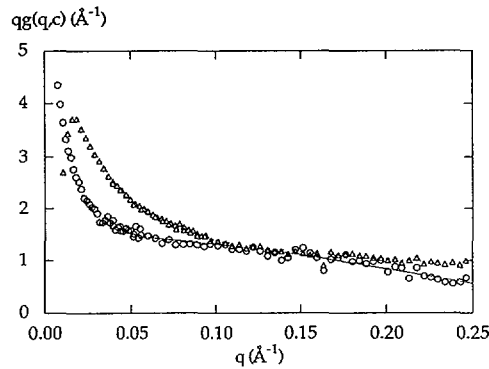


Fig. 6. — $qg(q, c)$ plots of PPA (Δ) and poly(2-octyne) (O) in deuterated toluene. Lines are the best fits by the theoretical structure factor $g_0(q) \Phi(q)$, the wormlike chain model is assumed for $g_0(q)$ (Ref. [21]). For PPA the mass per unit length used is $M_L = 39.1 \text{ g mole}^{-1} \text{ \AA}^{-1}$ corresponding to a *trans*-cisoid structure. The cross-section effect is modelled by $\Phi(q) = \exp(-q^2 R_c^2/2)$. The parameters are $L/b = 27$, $b = 46 \text{ \AA}$, $R_c = 3 \text{ \AA}$. For poly(2-octyne), the fit corresponds to a *trans*-transoid structure with $M_L = 45.3 \text{ g mole}^{-1} \text{ \AA}^{-1}$. An helical structure at local scale is used for $\Phi(q)$ (see text). The parameters correspond to the second serie given in the table.

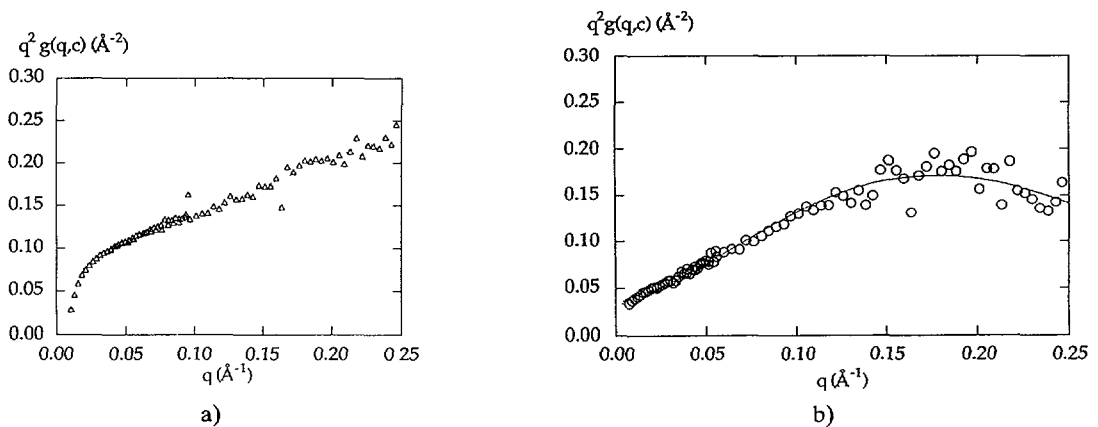


Fig. 7. — $q^2g(q, c)$ plots of the scattering function of PPA (7a) and poly(2-octyne) (7b). Symbols and fits are the same as for the figure 6.

similar to those observed for the polybutylthiophenes [14] or polydiacetylenes [7], that is it corresponds to a ribbon like structure, while poly(2-octyne) shows a pronounced decrease at $q \geq 0.2 \text{ \AA}^{-1}$, with a maximum located around 0.18 \AA^{-1}

3. Discussion.

3.1 CHAIN STRUCTURE.

3.1.1 PPA. — The $qq(q, c)$ plots of the two scattering curves show that the PPA chain is flexible while poly(2-octyne) shows a q^{-1} behavior at $q \approx 0.05 \text{ \AA}^{-1}$, thus it has a more rigid conformation. This can easily be deduced from figure 6 even without comparison to a theoretical structure factor.

The best fit for PPA measured at 5°C gives a statistical length $b = 45 \pm 5 \text{ \AA}$, suggesting a flexibility similar to that observed for polybutylthiophene [14]. The radius of gyration is $110 \pm 10 \text{ \AA}$.

PPA and polystyrene have almost identical monomer unit structures, the only difference being the conjugated backbone structure of PPA. Thus, from the difference between the statistical conformation of these two polymers one might expect to measure the effect of the electron delocalization on the chain conformation. On actuality, though, PPA is still flexible and the stiffness increase from conjugation is not more than a factor two.

The physical origin of the flexibility can be easily understood with the model we have already used [8, 9] and that we describe below (see paragraph 4). But, for the case of PPA, the flexibility could also be understood in another way. That is, we might argue that flexibility arises from a mixing of different conformers. For example, in a *trans*-cisoid structure, *trans*-transoid defects increase the chain flexibility. However, while not being able to eliminate such a possibility, one can note that R.R.S. results and neutron scattering data suggest mainly a *trans*-cisoid structure.

3.1.2 Poly(2-octyne). — A rigid behavior was observed for the poly(2-octyne) sample. Setting a plateau height at 1.48 in the Y.Y. model, we obtained good accordance between the computed values and the observed scattering curves (Figs. 6 and 7). The statistical length corresponding to the fit is $b = 135 \pm 10 \text{ \AA}$. Actually, the theoretical curve is obtained differently than by simply multiplying the computed structure factor by a constant such that the plateau height is reached. In what follows we will rationalize why at low q the plateau height is too high and why the decrease of the scattering intensity is more pronounced than for a ribbon-like structure.

3.1.3 Modelling of the cross-section. — More information on chain statistics can be obtained from a detailed analysis of the scattering curves at larger q values. It provides not only a more precise description of the actual shape of the cross-section, but also allows a better understanding of the whole scattering curve. Setting L_T as the total lateral extension of the chain and e as the width, a ribbon-like structure gives a q^{-2} dependence in the range $1/L_T < q < 1/e$ [7]. Since we do not observe such a behavior, we consider two other geometrical cross sections for describing the scattering curve at large q (Fig. 8). For a circular cross-section the function $\Phi(q)$ is given by :

$$\Phi(q) = \left(\frac{2 J_1(qR)}{qR} \right)^2 \quad (10)$$

where J_1 is the first order Bessel function and R is the radius of the cylinder. In the q range where the Guinier approximation applies (Eq. (8)), R_c is given by $R_c = R/\sqrt{2}$.

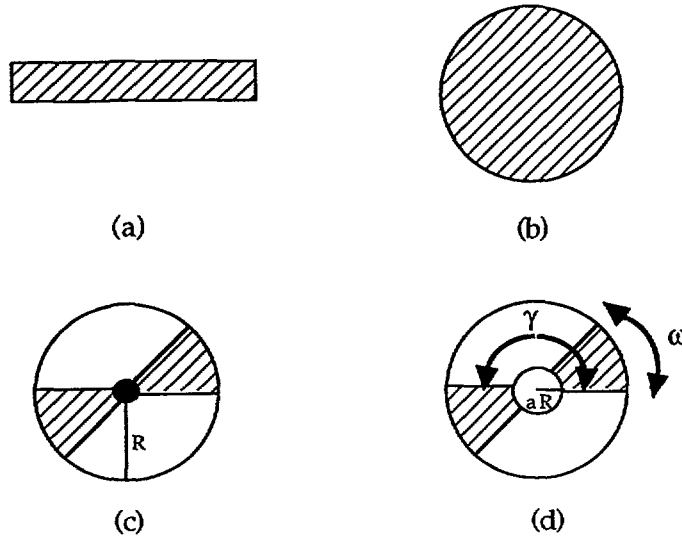


Fig. 8. — Simple geometrical forms describing the chain cross-section : ribbon (a), cylinder (b), helical structure (c), helical structure with central hollow part (d).

For a helical structure at the local scale, the results obtained by Pringle and Schmidt [26] can be used ⁽¹⁾ :

$$\Phi(q) = \frac{1}{H} \sum_{n=0}^{\infty} \varepsilon_n \cos^2(n\gamma/2) \frac{\sin^2(n\omega/2)}{(n\omega/2)^2} [g_n(qR, a)]^2 \tag{11}$$

where

$$g_n(qR, a) = 2 R^{-2}(1 - a^2)^{-1} \int_{aR}^R dr r J_n(qr \sqrt{1 - a^2}) \tag{12}$$

and with P the pitch length

$$\begin{aligned} q_n &= \frac{2 \pi n}{qP} & qR &> \frac{2 \pi nR}{P} \\ q_n &= 1 & qR &\leq \frac{2 \pi nR}{P} \end{aligned}$$

with $\varepsilon_n = 1$ for $n = 0$ and $\varepsilon_n = 2$ for $n \neq 0$. H is the length of the helix, R and aR are characteristic lateral lengths of the cross-section, while γ and ω describe the arrangement and width of the side groups (see Fig. 8). Two kinds of helical structure are considered, one without a central hollow region, the second with a central hollow region defining a spring-like structure. For the former case, the axial contour length is identical to the total contour length of the polymer. For the latter case, an effective scattering length density dependent on the geometrical parameters a , R and P must be considered. Let us define $L_w = \frac{M_w}{mu}$ as the total

⁽¹⁾ Note that the $\frac{\pi}{q}$ term given in reference [26] is already included in the function $g_0(q)$ (see (Eq. (7)), thus it has been dropped in (Eq. (12)). For the length H , see (Eq. (15)).

contour length ; for a helical-spring-like structure, the total contour length corresponds to the axis contour length and is given by :

$$L_w(a, R, P) = H = \frac{L_w}{\sqrt{\left[1 + \left(\frac{2\pi aR}{P}\right)^2\right]}} \quad (13)$$

Therefore, in the $g_0(q)$ term (Eq. (7)) the total contour length used in the Yoshizaki and Yamakawa model is given by equation (13) and not by $\frac{uM_w}{m}$. Also, instead of a plateau height A given by $\frac{\pi}{u}$, we have :

$$A = \frac{\pi}{u} \sqrt{\left[1 + \left(\frac{2\pi aR}{P}\right)^2\right]} \quad (14)$$

thus an increase of the scattering length density.

Equation (11) can be simplified in the case where $q \ll \frac{2\pi}{P}$. This corresponds to the scale at which the helical structure is approximated as a cylinder, i.e. the scale at which the helical structure appears as a homogeneous compact structure. For $q \ll \frac{2\pi}{P}$, we have only $q_n = 1$ except for $n = 0$, thus only the term with $n = 0$ remains in the serie (Eq. (11)). For $a = 0$, we recover the expression for the cylinder (Eq. (10)) and for $a \neq 0$ we have :

$$\Phi(q) = \sqrt{\left[1 + \left(\frac{2\pi aR}{P}\right)^2\right]} \left\{ \frac{2}{qR(1-a^2)} (J_1(qR) - aJ_1(aqR)) \right\}^2 \quad (15)$$

where the contour length has been dropped and included in the $g_0(q)$ term (Eq. (7)). Equation (15) emphasizes two main differences with respect to the cylinder case. One is given by the prefactor, which introduces an effective scattering length density, and a higher plateau height in the scattering vector range where the q^{-1} behavior is observed. The second concerns the scattering curve at large q . This effect can be more easily seen in a $q^2g(q)$ plot : the location of the maximum and the magnitude of the decrease are governed by a and R . For a given size of the substituent side-group the decrease is more pronounced for $a \neq 0$. The different theoretical curves obtained with equations (7), (8), (10), (15) are shown in figure 9. Also one can easily verify that equations (11) and (15) give the same results in the range of scattering vectors where equation (15) applies.

In figures 6 and 7b is reported the calculated structure factor corresponding to $b = 135 \text{ \AA}$, a pitch length $P = 15 \text{ \AA}$ and for the cross-section : $a = 0.17$, $R = 7.8 \text{ \AA}$ from which we obtain an actual length $\ell_c = 6.5 \text{ \AA}$ for the side-group. The parameters of the best fits obtained are given in the table. The calculated structure factors are almost identical for each monomer unit structure. The computed scattering functions differ only at scattering vectors higher than 0.17 \AA^{-1} , and even then the differences remain so small (within one percent) that we cannot expect to discriminate between the different structures.

All these parameter values are able to fit satisfactorily the whole q range. In any case, the statistical conformation is well described as a helical structure with a central hollow region. If the use of a trans-transoid conformation for the monomer unit allows one to obtain a good fit with different set of parameters, then one cannot eliminate the possibility of a *cis-transoid* (or *trans-cisoid*) conformation for poly(2-octyne). All series of parameters give a reasonable order of magnitude for the lateral dimension of the substituent side group : $\ell_c = 6$ or 6.5 \AA .

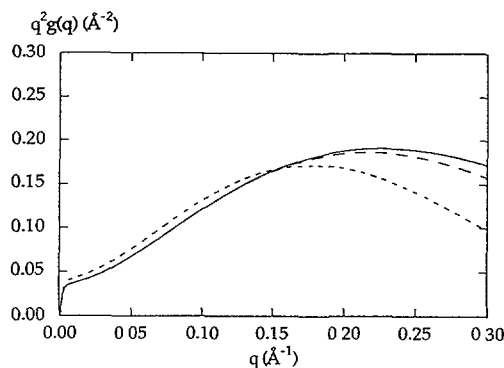


Fig. 9. — Theoretical structure factors $g(q) = g_0(q) \Phi(q)$. The input parameter corresponding to the scattering length density is the same for the three curves: $M_L = 45.3 \text{ g mole}^{-1} \text{ \AA}^{-1}$. The only change concerns the model of cross-section $\Phi(q)$ full line : Guinier approximation with $R_c = 4.6 \text{ \AA}$ (corresponding to $R = 6.5 \text{ \AA}$) (Eq. (8)), dashed line : circular cross-section $R = 6.5 \text{ \AA}$ (Eq. (10)), dotted line : helical structure with $a = 0.17$, $R = 7.8 \text{ \AA}$, $P = 15 \text{ \AA}$ (Eqs. (11) or (15)).

The inner radius lies between 1.3 \AA and 1.8 \AA . The *trans*-transoid conformer gives two values for the pitch length : $P = 15 \text{ \AA}$ corresponding to 7 monomer units per period and an average torsion between monomer units of about 51° , while the other fit gives $P = 20 \text{ \AA}$, thus 9 monomer units and an average torsion $\phi = 38^\circ$.

The scattering function at large q of the poly(2-octyne) sample differs markedly from the one observed for PPA in that a ribbon-like structure can be used for PPA. The mean square radius for the lateral extension is equal to $R_c = 3 \text{ \AA}$ consistent with a ribbon-model $\left(R_c^2 = \frac{L_T^2}{12} \right)$ in which the total lateral extension L_T is equal to 10 \AA , corresponding to phenyl rings distributed alternatively in both sides of the backbone.

4. Chain rigidity and optical properties.

The two substituted polyacetylenes differ in many ways : PPA has an optical transition at a much lower energy than poly(2-octyne) ; the statistical conformations are very different (the statistical length of poly(2-octyne) is about three times larger than the one of PPA), and the structure of the side group leads to completely different geometrical cross-sections of the chain.

If there are any relations between the first optical transition, the conjugation length, and the angular correlations along the backbone, one may first conclude that PPA shows more angular correlation (i.e. a more ordered structure) over the few units needed for allowing an optical absorption whose maximum is roughly located at 450 nm with a band edge up to 650 nm . This implies a decrease of the curvature fluctuation, thus a larger statistical length. On the contrary, the absorption spectrum of poly(2-octyne) suggests a π electrons configuration localized at the monomer unit scale. Thus, in as much as π electrons configuration bears on the average statistical conformation of the macromolecule, we expect similar statistical conformations to those observed for saturated polymers (i.e. a more flexible behavior). In fact, we just observed the opposite. This apparent contradiction is solved by taking explicitly into account the influence of the side-groups.

As for the scattering function : size effects and steric interference of the side-groups have an influence on the statistical conformation of the polymer chain in solution.

With a ground state defined as a rod conformation at 0 K, an isolated macromolecule has curvature fluctuations at finite temperature. For an infinitely thin thread, the curvature fluctuations are measured by the statistical length (20) :

$$b = \frac{2 \alpha}{k_B T} \quad (16)$$

where α is a constant characterizing the stiffness of the macromolecule.

For a chain with substituent side-groups, depending on the average lateral extension, a relatively large moment of inertia can change the magnitude of the curvature. Equation (16) is replaced by equation (17) [8] :

$$b = \frac{2 E \langle I_e \rangle}{k_B T} \quad (17)$$

where E is the elastic modulus and $\langle I_e \rangle$ is an average effective moment of inertia.

For a circular cross section, we simply have :

$$\langle I_e \rangle = \frac{\pi R^4 (1 - a^4)}{4} \quad (18)$$

For a ribbon-like structure (Fig. 10), the principal moments of inertia are $I_1 = \frac{a_1 a_2^3}{12}$ and $I_2 = \frac{a_2 a_1^3}{12}$. The steric repulsion between substituent side groups implies an average torsion along the backbone. The influence of the substituents can impose a helical structure corresponding to the propagation of the same sign of torsion between monomer units or a random distribution of torsion $\pm \phi$ along the backbone. In the latter case, the torsional fluctuations of the ribbon structure leads to an average effective moment of inertia (8) :

$$\langle I_e \rangle = \frac{1}{\phi} I_1 \int_0^\phi \sqrt{1 - k^2 \cos^2(\beta)} d\beta \quad (19)$$

where ϕ is the mean rotation between monomer units (Fig. 10) and $k^2 = 1 - (I_2/I_1)^2$. The two

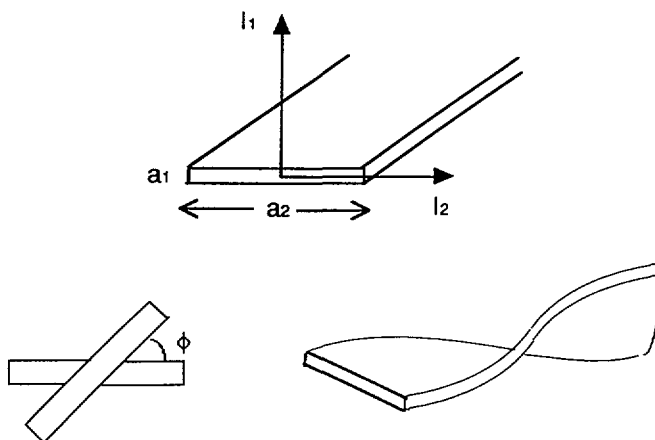


Fig. 10. — Sketch of the ribbon structure with the principal moments of inertia.

limiting cases are the planar ribbon structure ($\phi = 0$) and a $\pi/2$ rotation between neighboring monomer units. Equations (18) and (19) apply quite well to the polydiacetylene and polybutylthiophene cases [8, 9].

For PPA we can use equations (17) and (19) with $a_2 = L_T = 10 \text{ \AA}$ corresponding to the ribbon like structure (Fig. 11). For the poly(2-octyne), we again consider a very simple geometrical form, that is, side groups described as platelets but distributed only along one side of the backbone. In that case, we conjecture that we can again use our model because the torsion between the side-groups is large. We consider a segment length at a scale smaller than the statistical length $b = 135 \text{ \AA}$ such that the segment can be seen as a rod, and we look at the angular correlation of the vectors describing the pure torsion along the backbone. Using σ_i , the vector perpendicular to the rod at the position r_i , according to equation (5), one can define the persistence length λ_t related to a pure torsion :

$$\langle \sigma_1 \cdot \sigma_2 \rangle = \exp\left(-\frac{|\mathbf{l}_1 - \mathbf{l}_2|}{\lambda_t}\right). \quad (20)$$

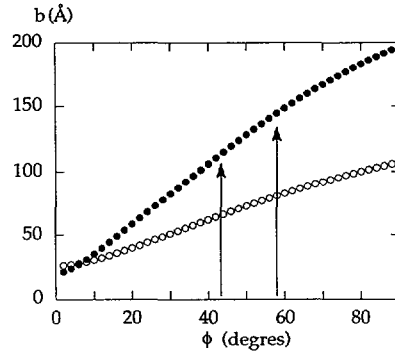


Fig. 11. — Variation of the statistical length as a function of the torsion ϕ between monomer units. Ribbon structure : $a_2 = 10 \text{ \AA}$ (O). Helical structure with $a = 0.17$, $R = 7.8 \text{ \AA}$ and $P = 15 \text{ \AA}$ (●). Arrows indicate the values corresponding to the torsion obtained for poly(2-octyne).

For n segments between the positions r_1 and r_2 , we have for a random distribution of torsion $\langle \sigma_1 \cdot \sigma_2 \rangle = \langle \cos(\phi) \rangle^n$ and λ_t is given by :

$$\lambda_t = \frac{a}{|\ln(\cos(\phi))|} \quad (21)$$

where ϕ is the torsion along the chain contour length responsible of the π -electron localization. For the present purpose, the statistical length b is defined with respect to the axis contour length ; this implies that we have to consider another rotation ϕ_a related to the helical axis. The relation between the two rotations can be obtain using a continuous approximation :

$$P \frac{d\phi_a}{d\ell} = \ell_p \frac{d\phi}{d\ell} \quad (22)$$

where ℓ_p is the chain contour length within the period P . The ratio ℓ_p/P is given by the square root term of the equation (14), so that we obtain the relation between the rotation ϕ along the chain and the rotation ϕ_a along the helical axis. For $\phi = 51^\circ$ we have $\phi_a = 58^\circ$ and $\lambda_t \approx 3.8 \text{ \AA}$, i.e. $\lambda_t \ll \lambda_b = b/2$. On the other hand, the π rotation for the side groups is

obtained for a length $P/2 = 7.5 \text{ \AA}$, i.e. $P/2 \ll b$. Therefore, within the length b the side groups are on average on both sides of the backbone (the statistical length b contains 18π torsion) such that the inertial contribution of the side groups to the local stiffness may be approximated with equation (19) and moments of inertia I_1 and I_2 given by :

$$I_1 = \frac{a_1 R^3 (1 - a^3)}{3}, \quad I_2 = \frac{a_1^3 R (1 - a)}{12} \quad (23)$$

Such a conjecture is reminiscent of the approximation used for the theoretical structure factor for $q < 2 \pi/P$. Here we assume that as long as $P \ll b$, we are able to calculate an average inertial contribution to the chain flexibility given by equations (19) and (23). In other words, this means that the helical structure is compact at the length scale of the curvature fluctuations.

For numerical applications, we use an elastic modulus $E = 10^{10} \text{ dyne cm}^{-2}$ and a thickness of the side groups $a_1 = 4 \text{ \AA}$. As discussed in the preceding papers [8, 9], 4 \AA is a reasonable value for a_1 , while the elastic modulus was chosen arbitrarily. This point is discussed below. The variations of b for different lateral lengths are reported in figure 11. These variations show both the effect of the size of the side groups and of the magnitude of the torsion.

We now try to estimate the statistical length using the values given by the fits of the scattering function. Two limiting cases are considered : one describing the chain as a cylinder with a central hollow region, the second using the average torsion deduced from the experimental results, but with a random distribution of the sign of the torsion along the backbone. This latter approach has the main interest to release the crude approximation describing the inertial contribution to the chain stiffness by a homogeneous dense cross-section.

The fit, obtained with $aR = 1.49 \text{ \AA}$ and $R = 7.5 \text{ \AA}$, leads for the cylinder structure (Eq. (18)) to $b = 250 \text{ \AA}$, while with equations (19) and (23) and $\phi = 58^\circ$, one obtains $\langle I_e \rangle = 0.55 I_1$ (Fig. 11) and $b = 146 \text{ \AA}$.

Nevertheless, this very good accordance between computed and observed values, if not accidental, may not be used as is. As noted above, the elastic modulus E was chosen arbitrarily and is one of the main parameters controlling the local stiffness (Eq. (17)). One cannot expect to have an accurate estimation of the effective elastic constant for a polymer coil in solution. It appears even more difficult for a polymer with substituents with corresponding steric repulsions between side groups. As a direct consequence, an accurate value of the magnitude of the rotation between monomer units cannot be obtained with our model. For example, for PPA the value deduced, $\phi = 26^\circ$, from the statistical length measured, $b = 46 \text{ \AA}$ (see Fig. 11), must be considered as an estimation. In addition, in that case the total extension of the side groups of about 10 \AA (the a_2 value) is not very large, thus providing a smooth variation of the statistical length as function of ϕ (Fig. 11), and therefore a larger uncertainty in the ϕ determination. Thus, we can only describe in general the behavior of macromolecules with substituents, without expecting to obtain in any case the right order of magnitude for the statistical length or for the average torsion in the case of a ribbon structure. What remains is that we are able to describe essential features for systems as diverse as substituted polydiacetylene, polythiophene and polyacetylene.

It is interesting to compare our results to the computed values of persistence lengths obtained by Rossi *et al.* [10]. Using torsional barrier heights obtained from octatetraene, they find $\lambda_t = 60 u$ and $\lambda_b = 112 u$ for the polyacetylene, that is a factor 40 for λ_t and 4 for λ_b with respect to the poly(2-octyne) results. The authors recalled that for soluble polyacetylene, such a computation may become irrelevant if substituent groups alter the potential of the planar structure. Here we note that poly(2-octyne) exhibits a torsion larger

than that calculated for polyacetylene, and does not lead to a corresponding increase in the curvature fluctuation. This emphasizes again the specific role of substituents on statistics of chains in solution.

There are numerous approaches to describe the effect of disorder on the π -electron structure. It is beyond the scope of this not to give an exhaustive list of the various attempts, but we shall recall a few of them. It is first interesting to note that a simple model considering resonant interactions between neutral excitations explains rather well the optical absorption observed on the oligothiophenes and polybutylthiophene in solution [27]. The two other main approaches are to use either *ab initio* calculations or semi-empirical models. In a general way, in a tight binding approximation, disorder will reduce the transfer integral (the bandwidth) and increase the gap.

Compared to the rod conformation, curvature fluctuations in flexible chains in solution induce a blue shift and a broadening of the visible absorption spectrum [3]. Therefore red shifts have been attributed to an increase in chain stiffness. This was the reason why color transitions observed for the polydiacetylenes (yellow to red (P4BCM) or yellow to blue (P3BCM)), were first explained as a single chain process : a coil to rod change [28].

Recently special attention has been devoted to disorder induced by torsional fluctuations, either by considering possible non linear excitations (which may be relevant to a description of the optical properties of polyaniline [13]) or by using a simple Hückel model, to establish a relationship between the optical absorption and the torsional fluctuation [10, 11]. If the first, lowest transition is directly related to the gap, any blue shift (red shift) corresponds to an increase (decrease) of the band gap. Modelling that behaviour was the basic aim of Rossi *et al.*

[10]. Using a band gap given by : $E_g = 2|\beta_d|(1 - \frac{\beta_s}{\beta_d} \langle \cos^2 \phi \rangle^{1/2})$ (where β_s and β_d are the transfer integral between the nearest neighbor sites for the single and double bonds), they calculated the average $\langle \cos 2 \phi \rangle$. The strong disorder limit where rotation acts as a chemical defect breaking the conjugation length [29, 30], was also considered.

The principal merit of the latter approach is that we do not need to relate directly the rigidity of the macromolecule to the π electrons delocalization. One can consider a rod conformation with large torsion between monomer units in which the π -electrons are confined at the monomer unit scale. The present work shows exactly this kind of behavior, the stiffer chain giving a transparent solution with an absorption maximum located in the U.V. range. Indeed, because of the existence of the substituent side groups, one may expect that solutions exhibiting color correspond to flexible conformations of polymers with the same backbone. This means that curvature fluctuation plays only a minor role or at least is not the pertinent parameter when torsion along the backbone occurs between monomer units.

On the other hand, direct comparison of the statistical conformation of PPA with the homologous saturated polystyrene chains does not show a sizeable enhancement of the chain stiffness. It has been predicted that the gain in energy due to electron delocalization either in the doped or neutral state can be so large that it could overcome the contribution of conformational entropy [4, 5]. Typically, one might consider that the contribution of the transfer integral β is about 1 eV, i.e. much more than kT . With a model based exclusively on π -electron interactions between units that fails to take into account the sterically induced torsion, Spiegel *et al.* [5] calculate a statistical length of about 150 monomer units, an order of magnitude larger than the one measured. Actually, R.R.S. studies found similar spectra in film and in solution, suggesting that the electronic structures are very close in both states. One may consider that steric interference between substituents controls the local order along the backbone regardless of its effect on the chain packing in the solid state or on the statistical conformation in solution. Therefore, it is quite difficult to estimate the exact influence of the

electron delocalization. Indeed, it becomes questionable as to whether it can be measured at all for soluble conjugated polymers within the current state of the science. Still, our present result shows at best a weak effect, if any.

5. Conclusion.

In this work we have tried to obtain quantitative information on the effect of torsion on chain conformation and π electrons configuration. With two substituted polyacetylenes, the present study shows unambiguously that, first, the average torsion is the main parameter controlling the statistical conformation of the polymer and second, it is also the driving parameter responsible for localization of π electrons. For one of the polymers, poly(2-octyne), the model used : an helical structure with a pitch length lying between 15 and 20 Å, enabled us to assign the order of magnitude of the average torsion that induces localization. The corresponding torsion destroys the backbone conjugation. The existence of the methyl group close to the backbone is clearly responsible for the average torsion, but does not result in a random torsion along the chain.

A natural continuation of this work would be to examine the effects of various substituents on chain structure with the aim of better controlling it [31], for example to obtain an helical-spring-like structure with a larger central hollow region and a smaller torsion along the backbone. Various efforts expanding on insights gained from the study of PPA and poly(2-octyne) structure are now in progress.

Acknowledgments.

We would like to thank Peter Timmins for his help during experiment, Institut Laue-Langevin for the beam time allocation and Mireille Adam for performing the light scattering study on poly(2-octyne).

References

- [1] EXARHOS G. J., RISEN W. M., BAUGHMAN R. H., *J. Am. Chem. Soc.* **98** (1976) 481.
- [2] SHAND M. L., CHANCE R. R., LE POSTOLLEC M., SCHOTT M., *Phys. Rev. B* **25** (1982) 4431.
- [3] SOOS Z. G., SCHWEIZER K. S., *Chem. Phys. Lett.* **139** (1987) 196.
- [4] PINCUS P. A., ROSSI G., CATES M. E., *Europhys. Lett.* **4** (1987) 41.
- [5] SPIEGEL D. R., PINCUS P. A., HEEGER A. J., *Synth. Met.* (Switzerland) **28** (1989) C385.
- [6] WENZ G., MÜLLER M. A., SCHMIDT M., WEGNER G., *Macromolecules* **17** (1979) 837.
- [7] RAWISO M., AIMÉ J. P., FAVE J. L., SCHOTT M., MULLER M. A., SCHMIDT M., BAUMGARTL H., WEGNER G., *J. Phys. France* **49** (1988) 861.
- [8] AIMÉ J. P., BARGAIN F., *Europhys. Lett.* **9** (1989) 35. For a review see AIMÉ J. P., Structural characterization of conjugated polymer solutions in the undoped and doped state in *Conjugated Polymers*, J.L. Bredas and R. Silbey Eds. (Kluwer Academic Publishers, Dordrecht, 1991) pp. 229-314.
- [9] AIMÉ J. P., RAMAKRISHNAN S., CHANCE R. R., KIM M. W., *J. Phys. France* **51** (1990) 963 ; AIMÉ J. P., GARRIN P., BAKER G. L., RAMAKRISHNAN S., TIMMINS P., *Synthetic Met.* **41** (1991) 859.
- [10] ROSSI G., CHANCE R. R., SILBEY R., *J. Chem. Phys.* **90** (1989) 7594.
- [11] VIALLAT A., ROSSI G., *J. Chem. Phys.* **92** (1990) 4548.
- [12] BREDAS J. L., HEEGER A. J., *Macromolecules* **23** (1990) 1150.
- [13] GINDER J. M., EPSTEIN A. J., *Phys. Rev. B* **41** (1990) 10674.
- [14] AIMÉ J. P., BARGAIN F., SCHOTT M., MÜLLER M. A., ECKHARDT H., ELSENBAUMER R. L., *Phys. Rev. Lett.* **62** (1989) 55.
- [15] MASUDA T., HIGASHIMURA T., *Adv. Polym. Sci.* **81** (1986) 121.

- [16] ABE Y., MASUDA T., HIGASHIMURA T., *J. Polym. Sci. Polym. Chem. Ed.* **27** (1989) 4267.
- [17] BATCHELDER D. N., BLOOR D., *Advances in Infrared and Raman Spectroscopy* **11**, R. J. H. Clark and R. E. Hester Eds., pp. 133-209.
- [18] OBERTHÜR R. C., I.L.L. internal report ;
RAGNETTI M., GEISER D., HÖCKER H., OBERTHUR R. C., *Makromol. Chem.* **186** (1985) 1701.
- [19] DES CLOIZEAUX J., JANNINK G., *Les polymères en solution, leur modélisation et leur structure* (Editions de Physique, les Ulis, France, 1987).
- [20] LANDAU L. D., LIFSHITZ E. M., *Stat. Phys.* 2nd Ed. (Pergamon Press, London, 1959) p. 478.
- [21] YOSHIKAWA T., YAMAKAWA H., *Macromolecules* **13** (1980) 1518.
- [22] DES CLOIZEAUX J., *Macromolecules* **6** (1973) 403.
- [23] *Small Angle X-ray Scattering*, O. Glatter and O. Kratky Eds. (Acad. Press., New York, 1982).
- [24] KOYAMA H., YOSHIKAWA T., EINAGA Y., HAYASHI H., YAMAKAWA H., *Macromolecules* **24** (1991) 932.
- [25] SEARS V. F., AECL-8490, Chalk River Nuclear Laboratories, Ontario, Canada (1984).
- [26] PRINGLE O., SCHMIDT P. W., *J. Appl. Cryst.* **4** (1971) 290.
- [27] FAVE J. L., to be published in *Electronics properties of polymers*, H. Kuzmany, M. Mehring, S. Roth Eds. (Springer, 1991).
- [28] SINCLAIR M., LIM K. C., HEEGER A. J., *Phys. Rev. Lett.* **51** (1983) 1768 and references therein.
- [29] SCHWEIZER K. S., *J. Chem. Phys.* **85** (1986) 1156.
- [30] SURJAN P. R., KUZMANY H., *Phys. Rev. B* **33** (1986) 2615.
- [31] CLOUGH S. B., SUN X. F., TRIPATHY S. K., BAKER G. L., *Macromolecules* **24** (1991) 4264.